Assessing the impact of upwind urbanization on the urban heat island effect of downwind areas a case study in Wuhan, China

Xuefan Zhou[1], Hong Chen[2]

[1] *Huazhong University of Science & Technology, Luoyu Road 1037, Wuhan, China, xuefanzhou@hust.edu.cn*

[2] *Huazhong University of Science & Technology, Luoyu Road 1037, Wuhan, China, chhwh@hust.edu.cn*

1. Introduction

Urbanization is one of the most extreme ways in which human activities change local land use and induce local land surface characteristics in urban areas that are substantially different from those in surrounding areas [1, 2]. The urban heat island (UHI) effect is one of the most significant phenomena caused by urbanization, and has been observed worldwide [3, 4]. According to the record, the urbanization rate of China had reached to 51.27% till 2011. By 2050, there is a potential that the urbanization rate of China may break through 70%. Therefore, Chinese major cities will maintain their expansions and growths in recent decades. That means if without precise planning and control, the UHI effects will become more and more serious in these cities. Urbanization will not only affect the urban itself on its UHI effect, as far as we know, the changes of urban morphology will cause its downwind rural areas' temperature to rise 0.5 to 1 °C in Wuhan, China[5]. Zhang et al. studied the urbanization impact in the Yangtze River delta and documented that in this area, the urbanization impact in summer is stronger and covers a larger area than that in winter because of the regional East Asian monsoon climate characterized by warm, wet summers and cool, dry winters [6]. Wang et al. also found that over the Beijing-Tianjin-Hubei area of China the change caused by urbanization in near surface temperature is most pronounced in winter, but the area influenced by focused on the regional influence of urbanization is slightly larger in summer [7].

Hence, this study selected a summer period with most significant UHI effect, and assessed the impact of upwind urbanization on the UHI effect of downwind areas. To quantitatively evaluate the impact, firstly, we selected two areas next to each other along the prevailing wind direction of Wuhan; then, we set 3 groups of 15 cases with different building densities, building heights, or green coverage ratios in the upwind area, and used Weather Research and Forecasting model of WRF to simulate each of the cases.

2. Methods and validation

WRF has been designed specifically for urban climate and environment studies, and is generally used in conjunction with the Urban Canopy Model (UCM**)** [8]. The urban canopy, which refers to the atmospheric layer from the land surface to the average building height in urban areas, significantly affects the urban boundary layer. The coupling of a mesoscale meteorology model with the UCM is based on a slab model, and additionally considers the effects of urban morphology and the building envelope on the heat balance in street canyons. The model also allows the simulation of urban thermodynamics, kinetic energy, thermal storage and the distribution of precipitation. Increasing numbers of researchers are using such combined models [9-11]. The WRF- UCM used in this study measures the effects of buildings in the urban canopy on heat gain and loss, and enters the results into an energy balance equation [12]. In addition, the UCM also considers the obstructive effects of buildings, the effects of turbulence around buildings, the multiple reflections of short- and long-wave radiation from building surfaces, and the sensible and latent heat fluxes from those surfaces.

We conducted sensitivity analysis of the WRF model by comparing the simulated and measured air temperature 2 m above ground level. The measurement data were obtained from a meteorological station (30.37°N, 114.08°W) located in a rural area of Wuhan City, as shown in Fig. 1.

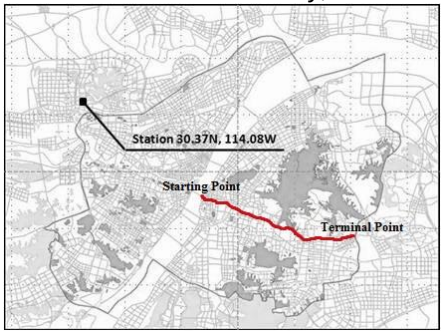

Fig. 1 Locations of the station (black) and the route (red)

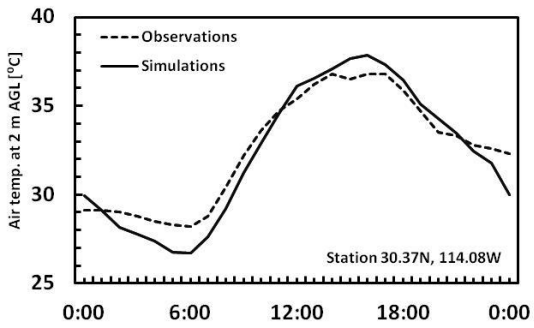

Fig. 2 Comparisons of observed and simulated T2

Fig. 2 compares the measured and calculated air temperatures on 26 July 2008, which differed in the period from 0000 Local Standard Time (LST) to 0800 LST, with a maximum difference of 1.56ºC at 0500 LST. Air temperature

differences should be attributed exclusively to anthropological heat in simulations because the temperatures of measured data are higher at night. The two sets of data coincided to a remarkable degree in other periods, with a minimum difference of 0.15ºC (at 1100 LST) observed. Mobile measurement was also conducted from 13-16 August 2011. The route of this measurement is indicated by the red curve in Fig. 1. Fig. 3 presents the results of the comparisons between the measured and calculated air temperature on 15 August 2011, with Figs. 3a and 3b showing the results at 1200 LST and 2100 LST, respectively. Although some of the points along the route show temperature differences greater than 1ºC, most are less than 1ºC. Remarkable similarities can be found between the increasing and decreasing trends of air temperature from the route's starting point to terminal point. The major differences in Fig. 3b were observed near the starting point, i.e. close to the riverside, at 2100 LST. The temperatures are higher in the measurement data than in the simulated data. The differences are primarily the result of the anthropogenic heat released by vehicles, which is difficult to properly simulate in the UCM, not to mention in the slab model. These results provided us with confidence in the model's efficacy as a predictive tool for our study.

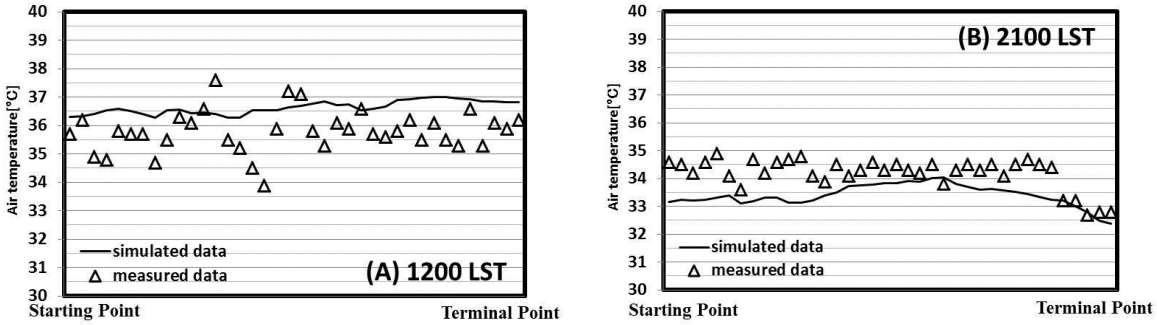

Fig. 3 Comparisons between the mobile measurement and simulation results of air temperature at (A) 1200 LST, (B) 2100 LST on 15 August 2011

3. Settings of numerical experiments

As shown in Fig. 4, Wuhan is the capital of Hubei Province in China. It is located at the confluence of the Han and Yangtze Rivers along the middle reaches of the latter. Wuhan occupies a land area of 8,494.41 km2, and has a population of 10,540,500. The city is famous for its vast area of inland water, which covers 2,217.6 km2, one-fourth its total area. Wuhan has a humid subtropical climate with abundant rainfall and four distinct seasons. The city experiences an extremely hot and humid summer, leading it to be known as one of the Three Boilers of China.

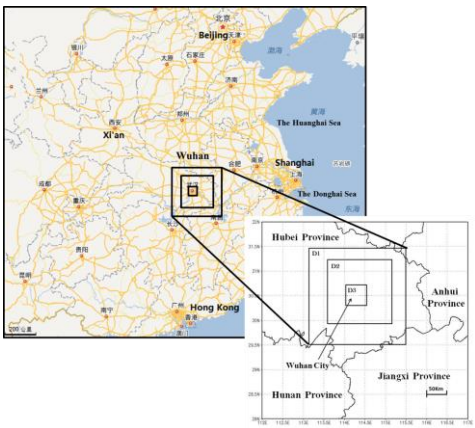

Fig. 5 Study area and domain settings

Table 1 Computational domains and grid arrangements

	Domain (X[km] x Y[km] x Z[km])	The number of grids	The size of grids (km)
D1	225x225 x 20	50x50x35	4.5
D2	150x150 x 20	100x100x35	1.5
D3	50x50 x 20	100x100x35	0.5

Table 2 Case settings (Average values)

Upwind Area		Building Height (m)	Building Density (%)	Greening Rate (%)
Impact of Building Height	Case_1	**9**	25	30
	Case_2	**18**	25	30
	Case_3	**27**	25	30
	Case_4	**36**	25	30
	Case_5	**45**	25	30
Impact of Building Density	Case_1	9	**25**	30
	Case_2	9	**30**	30
	Case_3	9	**35**	30
	Case_4	9	**40**	30
	Case_5	9	**45**	30
Impact of Greening Rate	Case_1	9	25	**20**
	Case_2	9	25	**25**
	Case_3	9	25	**30**
	Case_4	9	25	**35**
	Case_5	9	25	**40**
Downwind Area		**36**	**65**	**20**

USGS land-use and land-cover category 24 was applied to the geographic data used in this study. The simulations commenced at 1200 Universal Time, Coordinated (UTC) on 12 August 2011, and time integration was performed for 78 h. To clarify the impact of urban morphology on the urban climate and environment, the NECP/NCAR FNL global meteorological dataset supplied by the National Center for Atmospheric Research (NCAR) was applied to all cases. We set 3 domains as shown in Fig. 5; details of the domains are given in table 1.

We set 5 cases with different average building heights of upwind area from 9 m to 45 m; 5 cases with different average building density of upwind area from 25% to 45%; and 5 cases with different average greening rate of upwind area from 20% to 40%. No difference is set in downwind area among cases. Details of case settings are given in table 2.

4. Results

4.1 Impact of building height

We set 5 cases of different building heights from lowest (9m in case 1) to highest (45m in case 5) in the upwind area. Building heights of the 5 cases are the same in the downwind area. As shown in Fig. 6, the average surface temperature (TSK) of upwind area (Ave._U) slightly decreased (less than 1%), while the maximum TSK (Max._U) with distinct decreasing by about 3% and the minimum values (Min._U) by about 2% increasing. We assumed that the decreasing of the average and maximum TSK are due to the shading effect of tall buildings. Tall buildings provide street canyon with shades and thus lower the TSK during the daytime. However, much of the radiation absorbed by the upper part of high-rise buildings during the day is released into the street canyon in the hours during night, therefore, the minimum TSK increased.

Although the average and maximum TSK of upwind area decreased when the average building height increasing, the average, maximum, and minimum TSK of downwind area all increased (Ave._D, Max._D, and Min._D). There is no difference in the downwind area among these 5 cases, which illustrated that the changes of building heights of the upwind area distinctly affect the TSK of downwind area. The increasing of building heights of upwind area will change the volume and surface of artificial underlying, therefore, the upwind area will gain and save more heat energy. Due to the convection, heat transfer from upwind area to downwind area changes the heat balance of downwind area, thus, making the TSK there increase.

Shown in Fig.6b, the results of air temperature at 2 m height above ground (T2) of upwind area (U) and downwind area (D) are similar to TSK.

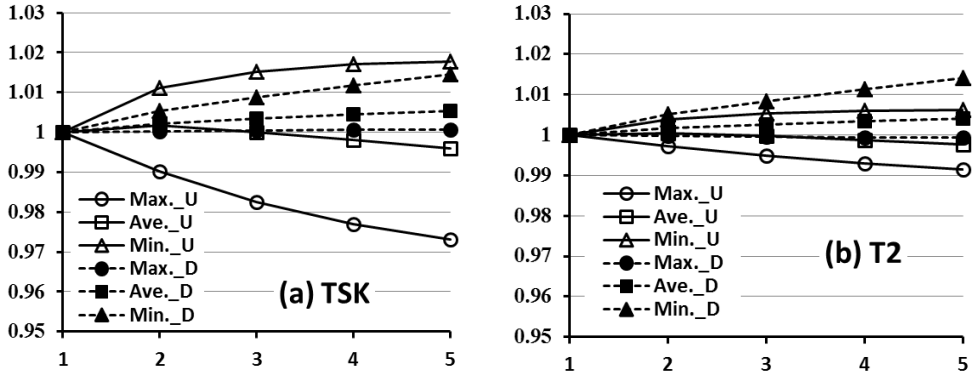

Fig. 6 Rate of increase of surface temperature (TSK) and air temperature at 2 m (T2) in relation to building height

4.2 Impact of building density

We set 5 cases of different building density from lowest (25% in case 1) to highest (45% in case 5) in the upwind area. Building density of the 5 cases are the same in the downwind area.

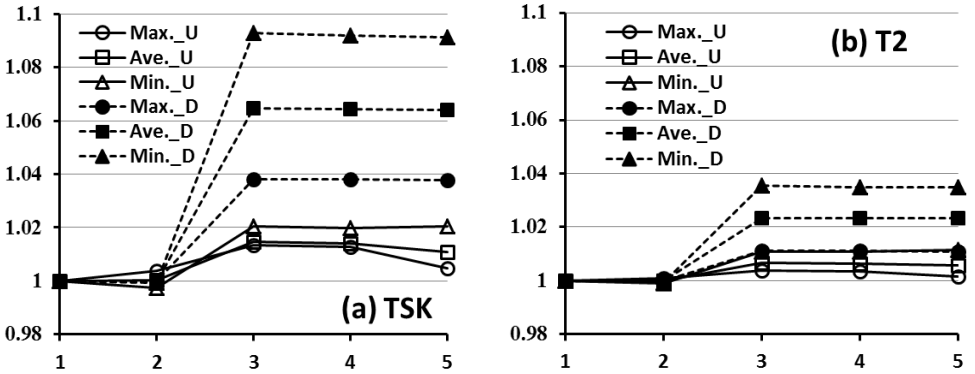

Fig. 7 Rate of increase of surface temperature (TSK) and air temperature at 2 m (T2) in relation to building density

As shown in Fig. 7, the TSK and T2 of upwind area are getting higher and higher while building density of that area increasing. A sharp increasing appears in case 3, when the average building density is reaching to 35%. Then when the building density is approaching to 45% in case 5, the TSK and T2 of upwind area slightly decreased. The TSK and T2 of downwind area are rising by much larger magnitude than of upwind area. Affected by the upwind area, the average TSK (Ave._D) of downwind area increased by about 6%, while, the minimum TSK (Min._D) increased by about 10% (5 times larger than upwind area).

To find out what cause the temperature of upwind area (Fig.8a) and downwind area (Fig.8b) to rise, we give the rate of increase of sensible heat flux (HFX), latent heat flux (LH), shortwave radiation (SWDOWN), long wave radiation-gain (GLW), long wave radiation-lost (OLR), ground surface heat flux (GRDFLX) and shown in Fig. 8. As shown, the ground surface heat flux (GRDFLX) of upwind area decreased by almost 6% when the building density grew from 25% to 45%. The sensible heat flux first increased, then slightly decreased after case 3 (35%). Therefore, we may assume that the increase of TSK and T2 of upwind area is caused by the increase of sensible heat flux and decrease of ground surface heat flux. As shown in Fig. 8b, the increase of TSK and T2 of downwind area is mainly caused by the increase of sensible heat flux. And these results illustrate that the temperature is rising because of the heat transfer from upwind area.

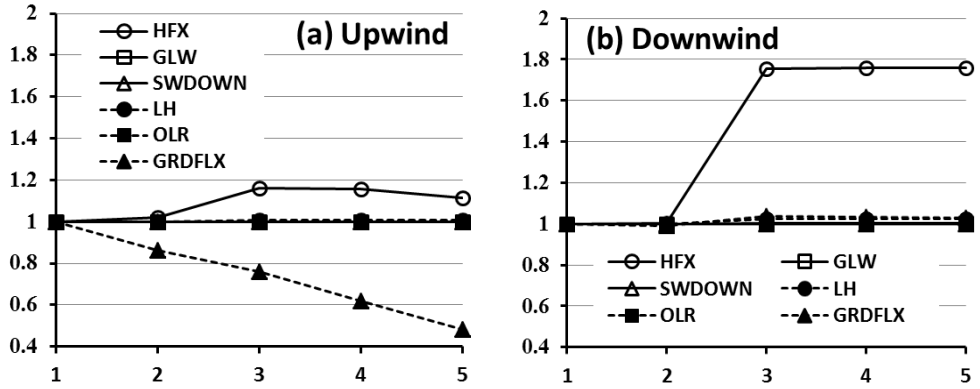

Fig. 8 Rate of increase of sensible heat flux (HFX), latent heat flux (LH), shortwave radiation (SWDOWN), long wave radiation-gain (GLW), long wave radiation-lost (OLR), ground surface heat flux (GRDFLX) in relation to building density

4.3 Impact of greening rate

As shown in Fig. 9, when the greening rate of upwind area increased, the average TSK and T2 dropped straightly, while the maximum TSK and T2 slightly decreased. We assumed that the decrease of temperature of upwind area is caused by the decrease of absorbed radiation. On the other hand, the increase of greening rate may increase the evaporation rate and transpiration rate in urban canopy, hence, increasing the latent heat flux and causing the temperature to drop in the upwind area. However, the changes of greening rate have limited impact on the TSK and T2 of downwind area.

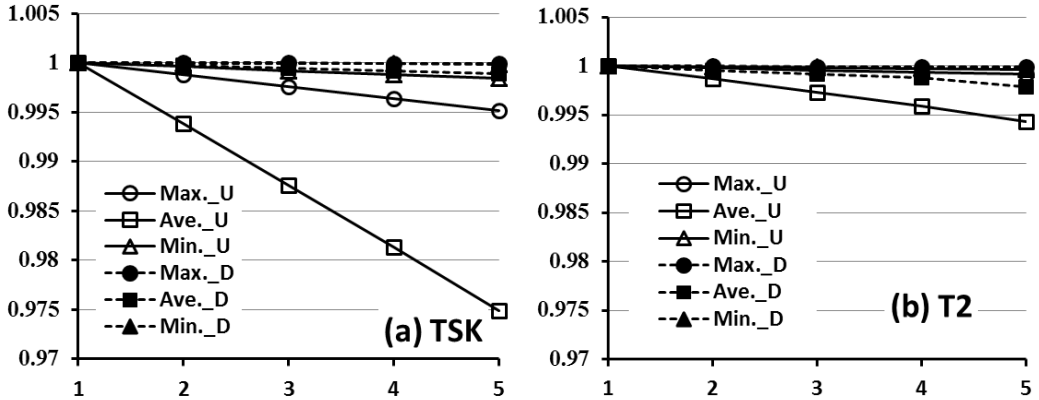

Fig. 9 Rate of increase of surface temperature (TSK) and air temperature at 2 m (T2) in relation to greening rate

5. Discussions

As shown in Fig. 10, we compared the impact of building height (HT), building density (DS), and greening rate (GC) of upwind area on the TSK and T2 of upwind area and downwind area. As for the TSK of upwind area, the impact of greening rate (GC) is larger than building density (DS), and the impact of building density (DS) is larger than building height (HT), which is GC> DS> HT. Moreover, the increase of building height and greening rate cause the TSK of upwind area to drop. The increase of building density causes the TSK of upwind area to rise; however, if the building density is higher than 35%, the TSK of downwind area slightly decreases. These regular patterns of impacts are similar in T2 of upwind area, except for, the impact on T2 is much smaller than TSK.

As for the TSK of downwind area, the impact of building density (DS) is larger than building height (HT), and the impact of building height (HT) is larger than greening rate (GC), which is DS> HT> GC. Moreover, the impact of building density increase on TSK of downwind area is 3 times larger than on TSK of upwind area. Besides, the increase of building height of upwind area causes the TSK of upwind area to drop, however, causes the TSK of downwind area to rise. These regular patterns of impacts are similar in T2 of downwind area, except for, the impact on T2 is much smaller than TSK.

As shown, the impact of building height (HT), building density (DS), and greening rate (GC) of upwind area on the

temperature of downwind area is larger than the temperature of upwind area. Especially, the building density (DS) of upwind area can be one of the major aspects, which cause the high temperature effect of downwind area; hence, we should control the building density well when planning.

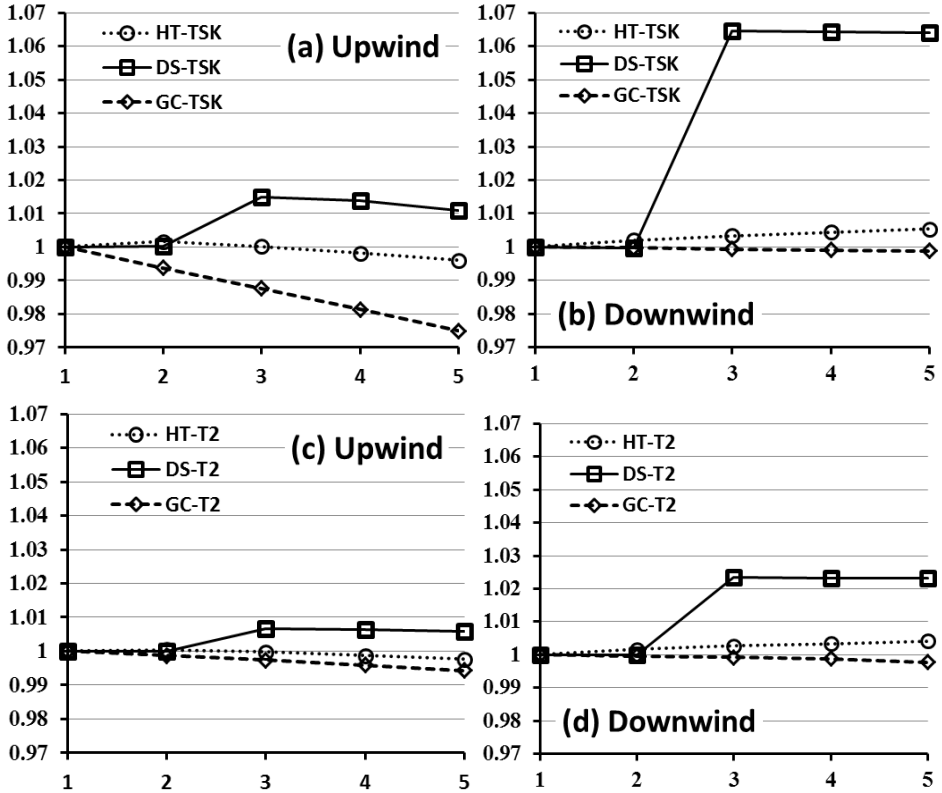

Fig. 10 Comparison of the impact of building height (HT), building density (DS), and greening rate (GC) of upwind area on the TSK and T2 of upwind area and downwind area

6. Conclusions

In this study, we set 5 cases with different average building heights of upwind area from 9 m to 45 m; 5 cases with different average building density of upwind area from 25% to 45%; and 5 cases with different average greening rate of upwind area from 20% to 40%. No difference is set in downwind area among cases. We compared the impact of building height (HT), building density (DS), and greening rate (GC) of upwind area on the TSK and T2 of upwind area and downwind area.

We found out that the increase of building height of upwind area causes the maximum and average TSK and T2 of upwind area to drop, while causing TSK and T2 of downwind area to rise. The TSK and T2 of upwind area are getting higher and higher while building density increasing. A sharp increasing appears when the average building density is reaching to 35%. Then when the building density is approaching to 45%, the TSK and T2 of upwind area slightly decreased. The TSK and T2 of downwind area are rising by much larger magnitude than of upwind area. After checking the energy balance of upwind area and downwind area, we found out that the increase of TSK and T2 of upwind area is caused by the increase of sensible heat flux and decrease of ground surface heat flux, and the increase of TSK and T2 of downwind area is mainly caused by the increase of sensible heat flux. And these results illustrate that the temperature is rising because of the heat transfer from upwind area. Moreover, we also found that the decrease of temperature of upwind area is caused by the decrease of absorbed radiation. On the other hand, the increase of greening rate may increase the evaporation rate and transpiration rate in urban canopy, hence, increasing the latent heat flux and causing the temperature to drop in the upwind area. However, the changes of greening rate have limited impact on the TSK and T2 of downwind area.

After comparing the impact of building height (HT), building density (DS), and greening rate (GC) of upwind area on the TSK and T2 of upwind area and downwind area, we noticed that as for the impact on the temperature of upwind area, GC> DS> HT, while, as for the impact on the temperature of downwind area, DS> HT> GC. With all the results of this study, we discovered that the building density (DS) of upwind area can be one of the major aspects, which cause the high temperature effect of downwind area; hence, we should control the building density well when planning.

Acknowledgment

This work was supported by National Nature Science Foundation of China (Grant No. 50978110), National Science and Technology Support Program (Grant No.2011BAJ03B03).

References

[1] Grimmond,C.S.B., J. A. Salmond, T. R. Oke, B. Offerle, and A. Lemonsu, 2004: Flux and turbulence measurements at a densely built-up site in Marseille: Heat, mass (water and carbon dioxide), and momentum. J. Geophys. Res., 109,

[2] Zhang N., Chen Y., 2014: A case study of the upwind urbanization influence on the urban heat island effects along the Suzhou-Wuxi corridor. American Meteorological Society, 53, 333-344.

[3] Childs, P. P., and S. Raman, 2005: Observations and numerical simulations of urban heat island and sea breeze circulations over New York City. Pure Appl. Geophys. , 162, 1955-1980.

[4] Gaffin, S. R., and Coauthors, 2008: Variations in New York City's urban heat island strength over time and space. Theor. Appl. Climatol., 94, 1-11.

[5] Zhou X., 2013: Research on the impact of urban morphology on urban climate in the built-up zone. Doctoral dissertation of Huazhong University of Science and Technology, 1-176.

[6] Hu, X. M., J. W. Nilesen-Gammon, and F. Q. Zhang, 2010: Evaluation of three planetary boundary layer schemes in the WRF model.J. Appl. Meteor. Climatol., 49, 1831-1844.

[7] Wang, M. N., X. Z. Zhang, and X. D. Yan, 2013: Modelling the climatic effects of urbanization in the Beijing-Tianjin-Hebei metropolitan area. Theor. Appl. Climatol., 113, 377-385.

[8] Fei Chen, Hiroyuki Kusaka, et. al., 2012: The integrated WRFurban modelling system development evaluation and applications to urban environmental problems. International Journal of Climatology, 31, 273-288.

[9] Yoichi Kawamoto, Ryozo Ooka., 2008: Development of urban climate analysis model using MM5 incorporating an urban canopy model. 5th Japanese-German Meeting on Urban Climatology, University of Freiburg, Germany. 10, 35.

[10] Sato, T., Murakami, S., Ooka, R., & Yoshida, S., 2008: Analysis of regional characteristics of the atmospheric heat balance in the Tokyo metropolitan area in summer. Journal of Wind Engineering and Industrial Aerodynamics, 96, 1640–1654.

[11] Trusilova, K., M. Jung, G. Churkina, U. Karstens, M. Heimann, and M. Claussen, 2008: Urbanization impacts on the climate in Europe: Numerical experiments by the PSU-NCAR Mesoscale Model (MM5). Journal of Applied Meteorology & Climatology, 47(5): 1442–1455.

[12] Sakakibara, Y., 1995: A Numerical Study of the Effect of Urban Geometry upon the Surface Energy Budget, Atmospheric Environment. 30, 487–496.